AGU PUBLICATIONS

JGR

Journal of Geophysical Research: Biogeosciences

RESEARCH ARTICLE
10.1002/2017JG003881

Key Points:
- Nitrate concentrations prior to the spring bloom are high throughout the water column over the entire Chukchi Shelf
- Nitrate concentrations are highest in the high-salinity winter water that advects into the Chukchi Sea from the Bering Sea
- Net community production estimates are higher than estimates from satellite but lower than those from prebloom nitrate in the Bering Sea

Correspondence to:
K. R. Arrigo,
arrigo@stanford.edu

Citation:
Arrigo, K. R., Mills, M. M., van Dijken, G. L., Lowry, K. E., Pickart, R. S., & Schlitzer, R. (2017). Late spring nitrate distributions beneath the ice-covered northeastern Chukchi Shelf. *Journal of Geophysical Research: Biogeosciences*, *122*, 2409–2417. https://doi.org/10.1002/2017JG003881

Received 6 APR 2017
Accepted 15 AUG 2017
Accepted article online 11 SEP 2017
Published online 18 SEP 2017

Late Spring Nitrate Distributions Beneath the Ice-Covered Northeastern Chukchi Shelf

Kevin R. Arrigo[1], Matthew M. Mills[1], Gert L. van Dijken[1], Kate E. Lowry[1,2], Robert S. Pickart[2], and Reiner Schlitzer[3]

[1]Department of Earth System Science, Stanford University, Stanford, CA, USA, [2]Department of Physical Oceanography, Woods Hole Oceanographic Institution, Woods Hole, MA, USA, [3]Alfred Wegener Institute for Polar and Marine Research, Bremerhaven, Germany

Abstract Measurements of late springtime nutrient concentrations in Arctic waters are relatively rare due to the extensive sea ice cover that makes sampling difficult. During the SUBICE (Study of Under-ice Blooms In the Chukchi Ecosystem) cruise in May–June 2014, an extensive survey of hydrography and prebloom concentrations of inorganic macronutrients, oxygen, particulate organic carbon and nitrogen, and chlorophyll *a* was conducted in the northeastern Chukchi Sea. Cold (<−1.5°C) winter water was prevalent throughout the study area, and the water column was weakly stratified. Nitrate (NO_3^-) concentration averaged 12.6 ± 1.92 μ*M* in surface waters and 14.0 ± 1.91 μ*M* near the bottom and was significantly correlated with salinity. The highest NO_3^- concentrations were associated with winter water within the Central Channel flow path. NO_3^- concentrations were much reduced near the northern shelf break within the upper halocline waters of the Canada Basin and along the eastern side of the shelf near the Alaskan coast. Net community production (NCP), estimated as the difference in depth-integrated NO_3^- content between spring (this study) and summer (historical), varied from 28 to 38 g C m^{-2} a^{-1}. This is much lower than previous NCP estimates that used NO_3^- concentrations from the southeastern Bering Sea as a baseline. These results demonstrate the importance of using profiles of NO_3^- measured as close to the beginning of the spring bloom as possible when estimating local NCP. They also show that once the snow melts in spring, increased light transmission through the sea ice to the waters below the ice could fuel large phytoplankton blooms over a much wider area than previously known.

1. Introduction

The Chukchi Sea sector of the Arctic Ocean is characterized by its broad and shallow continental shelf, inflow of water from the Bering Sea through Bering Strait (Woodgate et al., 2006), and seasonal but diminishing sea ice cover (Arrigo & Van Dijken, 2015). As a result of this loss of sea ice, phytoplankton abundance and rates of net primary production in the Chukchi Sea have increased by 20–30% in recent years, both in open water (Arrigo & Van Dijken, 2015; Belanger et al., 2013) and likely beneath the sea ice (Arrigo et al., 2012, 2014; Zhang et al., 2015).

The high productivity of the Chukchi Sea is maintained by the primarily northward flow of water through Bering Strait (Woodgate et al., 2006). Subsequent circulation on the Chukchi Sea shelf is controlled by bathymetry (Spall, 2007; Weingartner et al., 2005), with three primary flow pathways carrying water northward from the Bering Sea through Bering Strait (Figure 1) (Coachman et al., 1975; Spall, 2007; Weingartner et al., 2005; Winsor & Chapman, 2004). The western branch contains a large amount of nitrate-rich (~20 μ*M*) Anadyr Water (Sambrotto et al., 1984) and flows through Herald Canyon before exiting either to the north off the shelf break into the Canada Basin or to the east through Barrow Canyon (Weingartner et al., 2005; Winsor & Chapman, 2004). The eastern branch, referred to in summer as the Alaskan Coastal Current, is positioned relatively close to the coast and transports warm, fresh, but nutrient-poor Alaskan Coastal Water that originated in the Bering Sea and Gulf of Alaska (Cooper et al., 1997; Springer & McRoy, 1993; Walsh et al., 1989). The central branch flows between Herald Shoal and Hanna Shoal (through Central Channel) and transports a combination of Bering Shelf Water and Anadyr Water (Cooper et al., 1997; Hansell et al., 1993). These waters eventually migrate toward the Canada Basin (Lowry et al., 2015; Zhang et al., 2010), although some nutrients are regenerated locally on the shallow shelf (Codispoti et al., 2005).

By late spring or summer, the availability of nutrients in the northern Chukchi Sea, particularly dissolved inorganic nitrogen such as nitrate (NO_3^-) and ammonium (NH_4^+), is generally restricted to subsurface reservoirs

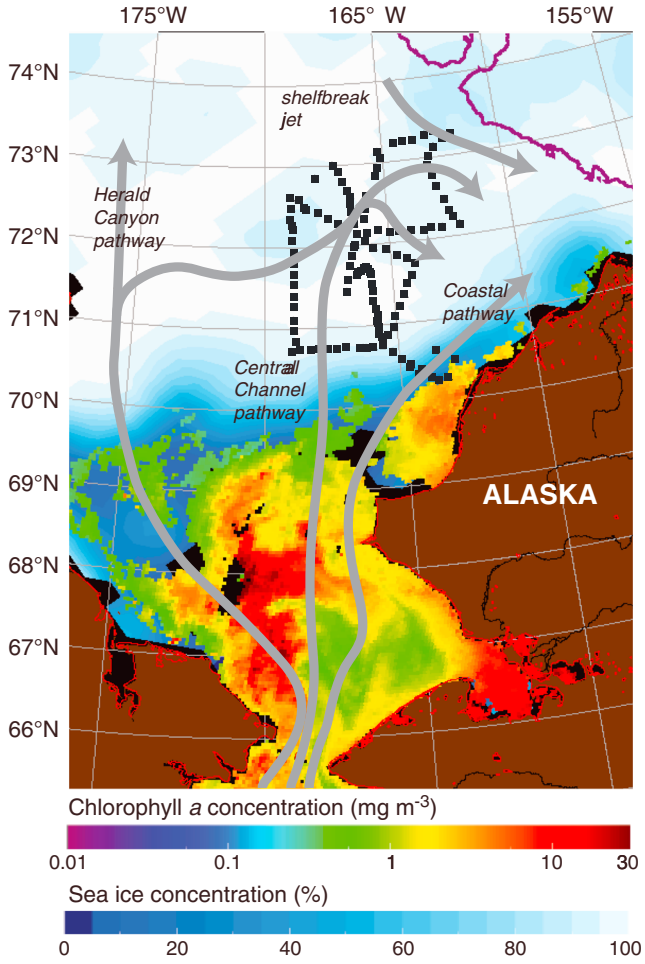

Figure 1. Map of the SUBICE study region showing the stations used in the study (black squares) overlaid on the concentration of chlorophyll *a* in open water and sea ice (calculated from the sea ice algorithm of Cavalieri et al. (1996)) on 15 June 2014. A schematic representation of the main flow paths of Pacific origin water on the Chukchi Shelf based on historical measurements are included (grey lines). The solid purple line denotes the 1000 m isobath.

of winter water (WW), which eventually limits phytoplankton growth (Codispoti et al., 2009; Cooper et al., 1997; Danielson et al., 2017; Lowry et al., 2015). This important summer nutrient resource is associated with the slower interior shelf pathways where WW has not yet flushed off the Chukchi Shelf into the Canada Basin (Lowry et al., 2015; Pickart et al., 2016). Farther south within the Chukchi Sea, open water blooms can remain prominent in spring and summer in waters exposed to nutrient-rich summertime Anadyr Water that enters through Bering Strait (Wang et al., 2005).

As phytoplankton deplete surface waters of nutrients, their growth rates at the depth of the nutricline eventually exceed those in near-surface waters, despite lower light levels. High ultraviolet radiation fluxes can also reduce algal growth in near-surface waters (Hessen et al., 2012). The result is that over the growth season, phytoplankton populations move deeper in the water column as light increases and the nitricline is progressively depressed, often forming a distinct subsurface chlorophyll maximum at depths of 20–40 m (Brown et al., 2015a; Danielson et al., 2017; Martin et al., 2010). Measurements of this progressive depletion of nutrients in surface waters have been used to estimate net community production (NCP), a quantity approximately equivalent to new production when the nutrient of interest is NO_3^- (Eppley & Peterson, 1979).

However, obtaining accurate estimates of NCP has been hampered by our poor understanding of prebloom baseline NO_3^- distributions on the Chukchi Shelf. The vast majority of nutrient data for this region has been collected during the summer and fall months when nutrient concentrations in surface waters are already reduced to growth-limiting levels (Codispoti et al., 2013; Danielson et al., 2017). The handful of nutrient samples obtained in the spring when substantial amounts of sea ice are still present suggest that the Chukchi Shelf is relatively well mixed prior to the initiation of the spring bloom, but the spatial coverage of these samples is extremely limited (Codispoti et al., 2005, 2009).

Here we present hydrographic data collected during the Study of Under-ice Blooms In the Chukchi Ecosystem (SUBICE) program in May–June 2014 (Figure 1). This is the most spatially extensive data set on prebloom nutrient distributions in the ice-covered northeastern half of the Chukchi Sea collected to date and can be used (1) to better understand nutrient cycling on the Chukchi Shelf, (2) to more accurately assess the relationships between WW, nutrients, and flow pathways, and as a baseline from which (3) to more accurately estimate net community production (NCP).

2. Methods

The SUBICE field campaign was conducted in the Chukchi Sea aboard United States Coast Guard Cutter (USCGC) *Healy* from 13 May to 23 June 2014. During the field expedition, the SUBICE team sampled the water column at 230 hydrographic stations, primarily on the continental shelf of the northeastern Chukchi Sea (Figure 1). Here we focus on 108 prebloom stations that were sampled within the ice pack during the early part of the cruise (18 May to 13 June). At each station, conductivity-temperature-depth (CTD) casts were made using dual temperature (SBE3), conductivity (SBE4c), and pressure (Digiquartz 0–10,000 psi) sensors attached to the 30 L, 12-position Niskin bottle rosette system. The CTD sensors underwent laboratory calibrations before and after the cruise, with calculated uncertainties of 0.001°C for temperature and 0.008 for salinity. Additional sensors on the rosette included dissolved oxygen (SBE43), photosynthetically active radiation (Biospherical QSP-2300), and fluorescence (WET Labs ECO-AFL/FL).

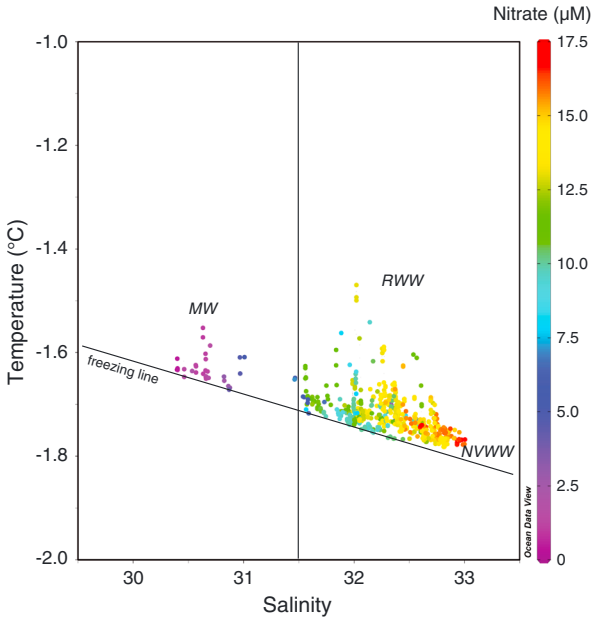

Figure 2. Potential temperature versus salinity diagram for stations shown in Figure 1. Colors denote nitrate concentration. MW = meltwater, NVWW = newly ventilated winter water, and RWW = remnant winter water.

Currents were measured using the ship's hull-mounted Ocean Surveyor 150 KHz (OS150) acoustic Doppler current profiler (ADCP) system. Because of the heavy ice, the data were not usable while the ship was steaming; hence, profiles were only obtained at the station sites. The data were processed following the procedure outlined in Pickart et al. (2016), which includes removing the barotropic tidal signal using the Oregon State University tidal model (http://volkov.oce.orst.edu/tides) (Padman & Erofeeva, 2004). The uncertainty in velocity is estimated to be <2 cm s^{-1}.

Discrete seawater samples were collected at a set of standard depths (2, 5, 10, 25, 50, 75, and 100 m) as well as at the depth of the subsurface fluorescence maximum (if present) and at 2–3 m above the seafloor. Nutrient analyses were performed on board the ship with a Seal Analytical continuous flow Auto-Analyzer 3 using a modification of the method described in Armstrong et al. (1967) to measure the concentrations of nitrate (NO_3^-), ammonium (NH_4^+), nitrite (NO_2^-), phosphate (PO_4^{3-}), and silicate ($Si(OH)_4$). Seawater samples for dissolved oxygen (O_2) were analyzed using standard Winkler titrations to calibrate sensor measurements from the CTD casts. For analysis of chlorophyll *a* (Chl *a*) concentration, seawater was filtered onto 25 mm Whatman glass fiber filters (GF/F, 0.7 μm nominal pore size). Filters were extracted in the dark in 5 mL of 90% acetone for 24 h at +3°C prior to measurement (Holm-Hansen et al., 1965) on a Turner Designs 10-AU fluorometer calibrated with pure Chl *a* (Sigma-Aldrich). Particulate organic carbon and nitrogen (POC and PON) samples were filtered through precombusted 25 mm GF/Fs. Blank filters were made daily by passing ~25 mL of filtered (0.2 μm) seawater through GF/Fs and processing them the same as for the particulate samples. All filters were immediately dried at 60°C and stored dry until processing. Prior to analysis, samples were fumed with concentrated HCl, dried in a low-temperature oven at 60°C, and packed into tin capsules (Costech Analytical Technologies, Inc.) for analysis. Samples were analyzed on an Elementar vario EL cube or MICRO cube elemental analyzer (Elementar Analysensysteme GmbH, Hanau, Germany) which was interfaced to a PDZ Europa 20-20 isotope ratio mass spectrometer (Sercon Ltd., Cheshire, UK). Calibration standards were glutamic acid and peach leaves.

The calculation of NCP from nutrient deficits assumes that water masses move as a single parcel. Thus, at any particular location, surface water NO_3^- concentrations at the time of sampling are a function of initial starting values in early spring before the phytoplankton bloom begins and any phytoplankton uptake that has taken place since that time. Water that advects into the Chukchi Sea during spring/summer will have its own NO_3^- depletion signature resulting from NCP that took place outside our study region and would cause an overestimation of local NCP. However, because the residence time on the shelf (Spall, 2007; Winsor & Chapman, 2004) is longer than the phytoplankton bloom, this error is likely to be small (see section 5 below). NCP was calculated by using our prebloom NO_3^- concentration profiles on the Chukchi Shelf as a baseline and using data from historical summer cruises (Arrigo et al., 2014; Codispoti et al., 2005, 2009; Danielson et al., 2017; Lowry et al., 2015; Mills et al., 2015) to the region to determine the depth of the nitricline, then assuming that NO_3^- concentrations above that depth were reduced to zero. The vertical integral of NO_3^- depletion was then assumed to be equal to NCP, which was converted to carbon (C) units assuming a molar C:N uptake ratio of 6.0 to be consistent with previous estimates by Hansell et al. (1993).

3. Prebloom Hydrography

Most of the SUBICE study was conducted in shallow (40–50 m) continental shelf waters that were covered by 1.0–1.5 m of sea ice and 0.02–0.15 m of snow. Sea ice concentrations were determined by 2-hourly ship observations and passive microwave satellite data at each station during our study and were all approximately 100% (Figure 1). The surface melt ponds that are common in this area in summer (Arrigo et al.,

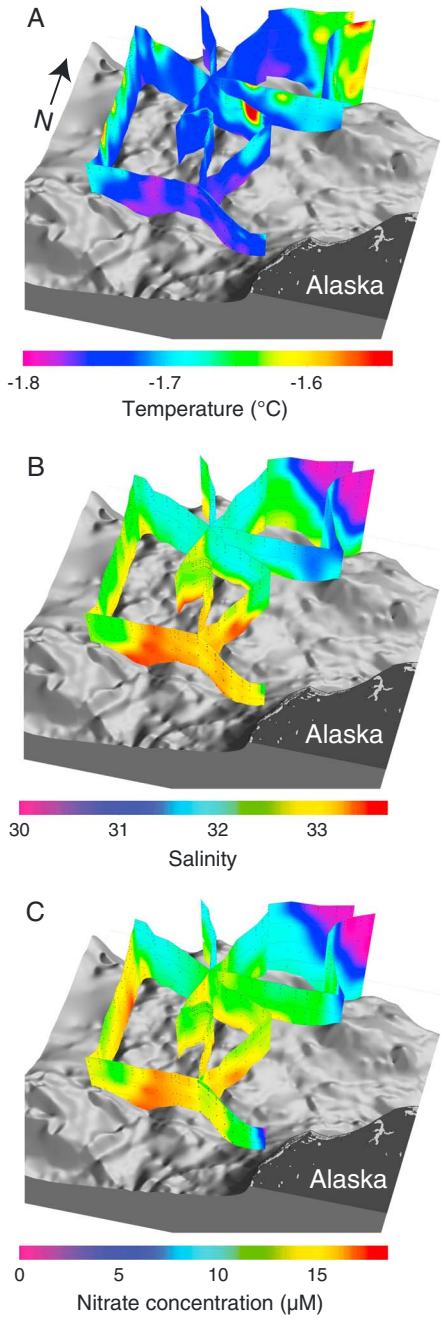

Figure 3. Three-dimensional sections of (a) potential temperature, (b) salinity, and (c) nitrate concentration for a subset of the SUBICE station grid. Only stations sampled early in the season prior to appreciable phytoplankton growth have been included. Graphics created using Ocean Data View and Ocean3D.

2014) were absent during our study due to persistently subfreezing air temperatures (see also Pacini et al., 2016).

Over much of the northeast Chukchi Shelf, seawater temperature and salinity fell within a narrow range of −1.78°C to −1.55°C and 32 to 33, respectively (Figure 2), demonstrating that in the late spring, the shelf is composed almost exclusively of WW (Carmack, 2000). At the northernmost stations sampled near the shelf break, waters were similarly cold but much fresher (salinity of 30.5 to 32) than on the shelf, indicating the presence of early-season meltwater and/or low-salinity coastal or Canada Basin waters that had advected into the sampling region (MW). Remnant winter water (RWW) was also found seaward of the shelf break. This water mass is one of the main constituents of the cold halocline of the Canada Basin (Anderson et al., 2013). In the southern part of our study domain, beneath the pack ice, the water was close to the freezing point over a range of salinities. This is referred to as newly ventilated winter water (NVWW), having been formed during the preceding winter. Temperature (Figure 3a) and salinity (Figure 3b) sections indicate that shelf waters were two layered but weakly stratified in most areas.

Mean oxygen saturation (80–85%) and concentrations of Chl *a* (<1 mg m^{-3}), POC (<60 mg m^{-3}), and PON (<70 mg m^{-3}) were generally low on the shelf beneath the ice, indicating that the phytoplankton bloom had not yet begun in waters beneath the sea ice during the early part of the cruise.

Nitrate (NO_3^-) concentrations under the ice exceeded 8 μ*M* virtually everywhere on the shelf and were highly correlated with salinity (Figure 4, $R = 0.84$), except for the far eastern and northern regions of our study area where nutrient concentrations were very low in the basin and near the coast (Figure 3c). Over much of the shelf, the weakly stratified water column had surface and near-bottom NO_3^- concentrations that averaged 12.6 ± 1.92 μ*M* and 14.0 ± 1.91 μ*M*, respectively. Concentrations of PO_4^{3-} and $Si(OH)_4$ exhibited spatial patterns (not shown) similar to that of NO_3^-, with mean springtime concentrations of 1.86 ± 0.15 and 48.5 ± 5.59 μ*M*, respectively, on the shelf. NH_4^+ concentrations on the Chukchi Sea shelf were also relatively high but spatially more variable than other nutrients, averaging 1.57 ± 0.51 μ*M*. The mean NO_3^-:PO_4^{3-} and NO_3^-:$Si(OH)_4$ ratios in our study region were 9.16 and 0.27, respectively. These prebloom nutrient ratios are consistent with those measured in near-bottom shelf waters later in the season, prior to the depletion of NO_3^- in surface waters that marks the end of the spring bloom (Codispoti et al., 2009, 2013; Cooper et al., 1997; Danielson et al., 2017), and are indicative of a NO_3^--limited system.

The only other available springtime data that we are aware of to which we can compare these NO_3^- concentrations were made during the Shelf Basin Interaction (SBI) program in 2002 and 2004 (Codispoti et al., 2005, 2009). Only a few stations were sampled during SBI in the month of May up on the continental shelf away from the shelf break (Figure 5), but reported NO_3^- concentrations were in good agreement with our measurements made at a similar time and place during SUBICE. Vertical profiles show that NO_3^- concentrations during SBI were generally uniform with depth and ranged from 10 to 15 μ*M* within our study region. There was also some evidence of slight near-bottom enhancement of NO_3^- concentration (Figure 5), similar to what we observed during SUBICE. Salinity versus NO_3^- regressions from both studies suggest that NO_3^- concentration might have been slightly higher during SUBICE than during SBI, with

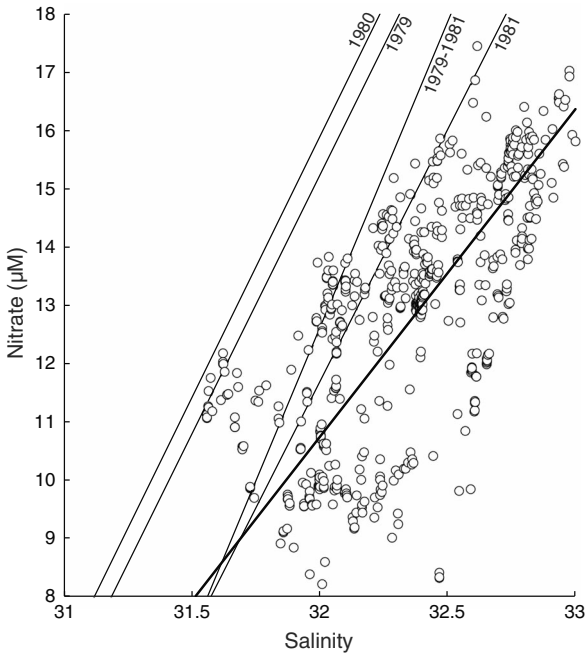

Figure 4. Relationship between nitrate concentration and salinity for stations shown in Figure 3. Dark black line is the linear fit of the data ($y = 5.631x - 169.47$, $R = 0.84$, $p < 0.001$). Light black lines are the regressions of nitrate versus salinity for three different years (and all 3 years combined) from the southeastern Bering Sea (Hansell et al., 1993), illustrating generally higher nitrate concentrations than observed in the northeastern Chukchi Sea during our study.

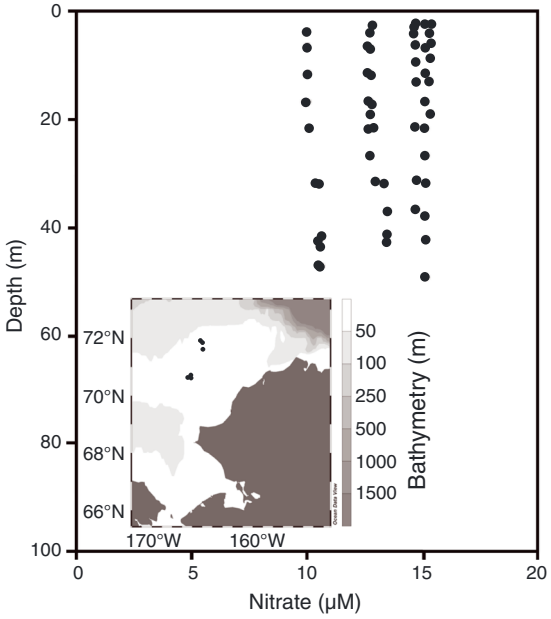

Figure 5. Nitrate profiles obtained on the Chukchi Sea shelf in May of 2002 and 2004 during the Shelf-Basin Interactions program. Inset map shows station locations and bathymetry.

NO_3^- concentrations at a salinity of 33 for the two studies of 16.4 and <15, respectively (Codispoti et al., 2005, 2009).

Although springtime NO_3^- concentrations were high almost everywhere on the shelf during SUBICE, those along the main flow paths across the Chukchi Sea shelf (e.g., the Central Channel jet), which were identified based on ADCP data, were generally 3–5 μM higher than concentrations in the surrounding areas (Figure 3c). Consistent with previous studies (Pickart et al., 2016; Weingartner et al., 2013), we found that the Central Channel pathway is augmented by flow from the west (likely from Herald Canyon) and, upon encountering Hanna Shoal, the pathway bifurcates. Maximum velocities within these jets (0.20–0.25 m s^{-1}) are higher than velocities over the rest of the shelf and carry a higher fraction of high NO_3^- Anadyr Water from the Bering Sea, consistent with their relatively high salinity (Figure 3b) (salinity = 32.5–33.0) (Coachman et al., 1975). However, in the waters adjacent to the jets, NO_3^- concentrations were also generally in excess of 10 μM. Convective overturning was likely taking place during our survey within small leads in the pack ice, as demonstrated by Pacini et al. (2016) who used a polynya model in conjunction with a 1-D mixing model to show that the water column on the interior shelf would overturn in a matter of hours subject to the observed air-sea forcing during the first part of our survey. This implies that the convective mixing would stir regenerated nutrients from the seafloor into the upper water column. Hence, the generally high NO_3^- concentrations observed throughout our study region, including those outside of the main flow pathways, indicate that local NO_3^- sources augment the nutrients that are transported through Bering Strait.

4. Estimates of NCP

Surface water concentrations of NO_3^-, PO_4^{3-}, and $Si(OH)_4$ on the Chukchi Shelf measured in spring during SUBICE were much higher than those measured later in the season in the same region (Arrigo et al., 2014; Codispoti et al., 2005, 2009; Danielson et al., 2017; Hansell et al., 1993; Lowry et al., 2015), due to nutrient assimilation by phytoplankton during the summer blooms. Therefore, the horizontal distribution of prebloom NO_3^- concentrations measured during SUBICE can be used with nitricline depth measured later in the season to determine minimum estimates of NCP on the Chukchi Sea shelf (they are minimum estimates because they do not account for possible additions of NO_3^- to the system during the growing season). Summer cruises to the Chukchi Sea have shown that NO_3^- is fully depleted by phytoplankton down to an average depth of 30 m by mid-July, even in areas where sea ice concentration was near 100% (Arrigo et al., 2012, 2014; Brown et al., 2015a; Danielson et al., 2017; Lowry et al., 2015; Varela et al., 2013). Given the prebloom NO_3^- concentrations we measured in the upper 30 m, this yields a mean NCP estimate of 27.8 ± 4.13 g C m^{-2} a^{-1}.

Because phytoplankton growth and nutrient consumption continue to erode the nitricline after mid-July (Brown et al., 2015a; Codispoti et al., 2005), the above value for NCP probably

underestimates the annual value. Therefore, we also computed NCP from our prebloom NO_3^- data using two further assumptions, (1) that NO_3^- was completely consumed within the upper 40 m of the water column during summer and (2) that NO_3^- was completely consumed throughout the entire ~50 m water column (this represents an unlikely, but maximum possible, estimate for local NCP from NO_3^- deficits). Our data suggest that if the nitricline were to deepen to 40 m, time- and depth-integrated NCP would increase by 35% to 37.6 ± 5.59 g C m^{-2} a^{-1}. If prebloom NO_3^- is fully consumed throughout the water column on the shallow shelf, NCP only increases by another 12.5%, to 42.3 ± 6.89 g C m^{-2} a^{-1}. These mean estimates of NCP do not include the low values measured in the northern Chukchi Sea near the shelf break (5–20 g C m^{-2} a^{-1}) that are associated with the persistently low NO_3^- waters of the Canada Basin (Codispoti et al., 2013).

Our NCP values are on the low end of previous estimates for the southern (40–70 g C m^{-2} a^{-1}) and western (70 g C m^{-2}) Chukchi Sea (Codispoti et al., 2013; Hansell et al., 1993; Mills et al., 2015) made using the same approach. Given the relatively low sensitivity of the NCP calculation to the nitricline depth, the primary reason for these NCP differences is that previous studies assumed higher prebloom NO_3^- concentrations than those used here that were based either on a small amount of data collected in the Chukchi Sea (Mills et al., 2015) or measurements from far upstream in the Bering Sea (Hansell et al., 1993). For example, Hansell et al. (1993) estimated NCP using prebloom NO_3^- values that were calculated from a regression between NO_3^- concentration and salinity obtained for waters of the southeastern Bering Sea. This regression yielded a NO_3^- concentration of 23.2 μM at a salinity of 33, much higher than the mean prebloom value of 16.4 μM NO_3^- we measured at that same salinity on the northeastern Chukchi Sea shelf (Figure 4). Because both of our studies assume complete nutrient depletion down to the nitricline by the end of summer, the higher initial NO_3^- concentrations in Hansell et al. (1993) would yield larger NO_3^- deficits and thus greater estimates of NCP in the southern and western Chukchi Sea.

5. Considerations for Measuring NCP From Nutrient Deficits

There are three difficulties inherent in estimating local NCP from measured nutrient deficits on an inflow shelf like the Chukchi Sea (Carmack & Wassmann, 2006). First, it is difficult to define prebloom NO_3^- concentrations because of interannual differences in relative amounts of nutrient-rich Anadyr Water and nutrient-poor Alaskan Coastal Water entering the Chukchi Sea and their spatial redistribution on the shelf. This water mass variability is linked to interannual differences in the prevailing wind fields (Danielson et al., 2017) and likely alters prebloom nutrient inventories on the Chukchi Sea shelf. While interannual variability in prebloom NO_3^- concentration explains some of the difference between the two NCP estimates, its role is probably small because SUBICE values for WW NO_3^- are consistent with WW values published previously for the same area of the Chukchi Sea in 2002 and 2004 (Figure 5) and in 2010 and 2011 (Lowry et al., 2015; Mills et al., 2015). This suggests that spatial differences in prebloom NO_3^- between the Chukchi Sea and Bering Sea shelves have a larger impact on the estimate of NCP than interannual variability in prebloom NO_3^- within the Chukchi Sea.

Second, N-cycle processes other than phytoplankton uptake alter inventories of NO_3^- as water flows over the shallow Bering and Chukchi Sea shelves. Much of the 6.8 μM difference in prebloom NO_3^- concentration at a salinity of 33 between Anadyr Water in the southeastern Bering Sea (23.2 μM) and on the Chukchi Sea shelf (16.4 μM) is likely due to an imbalance between the processes that alter NO_3^- concentrations during transit between the two regions. For example, the microbial conversion of NO_3^- to nitrogen gas via sediment denitrification results in a significant loss of fixed N on both the Bering and Chukchi Sea shelves (Chang & Devol, 2009; Devol et al., 1997; Granger et al., 2011; Haines et al., 1981; Koike & Hattori, 1979; Mills et al., 2015; Tanaka et al., 2004). Furthermore, the sediments of the Bering and Chukchi Sea are sites of active coupled partial nitrification-denitrification (Granger et al., 2011), while the deeper portions of the water column are sites of nitrification (Brown et al., 2015b; Hartnett, 1998; Henriksen et al., 1993), resulting in the regeneration of NO_3^- from ammonified organic N. The net 6.8 μM decrease in NO_3^- between the Bering and Chukchi Seas indicates that losses of NO_3^- through denitrification outweigh the gains from nitrification, which must be accounted for when estimating NCP using nonlocal prebloom NO_3^- values.

Finally, estimation of local NO_3^- deficits is complicated by the continued inflow of waters carrying NO_3^- deficit signals into the northeastern Chukchi Sea from phytoplankton blooms within ice-free waters to the south,

either in the northern Bering Sea (Brown et al., 2015b) or the southern Chukchi Sea (Figure 1). The same is true for NO_3^--depleted waters from the Canada Basin that are transported onto the Chukchi Shelf through upwelling (Aagaard & Roach, 1990; Bourke & Paquette, 1976; Pickart et al., 2009). During our SUBICE cruise, we first observed NO_3^--depleted waters beneath fully consolidated sea ice and snow in the narrow but rapidly flowing midshelf jet that had penetrated into the sea ice zone, reaching as far north as 71.4°N by 18 June. While adjacent areas of the shelf were much less impacted, advection of this reduced NO_3^- water into our study region will markedly alter estimates of local NCP.

Clearly, estimates of initial NO_3^- concentrations used in NCP calculations for a given region should be based on local profiles of NO_3^- measured as close to the beginning of the spring bloom as possible. How close depends on the length of phytoplankton bloom relative to the residence time of water on the Chukchi Sea shelf. If the phytoplankton bloom is short lived relative to the residence time of NO_3^- on the shelf, then prebloom NO_3^- can be measured either earlier in the season or farther upstream to obtain accurate estimates of NCP. Satellite ocean color data show that the amount of time it takes for phytoplankton in the Chukchi Sea to increase from prebloom to peak bloom Chl *a* concentrations is approximately 1 month (Arrigo & Van Dijken, 2011). Given that the timing of peak biomass during a bloom generally coincides with the exhaustion of surface NO_3^- (Alkire et al., 2012) the relevant timescale for measuring NCP on the Chukchi Sea shelf is approximately 1 month. This is because any phytoplankton growth after this time would be dependent on recycled nutrients and therefore would not contribute to NCP.

Based on numerical models of the Chukchi Sea (Spall, 2007; Winsor & Chapman, 2004), the residence time of Pacific water within our study domain on the northeast shelf is anywhere from a couple of months to a half year, substantially longer than the length of the phytoplankton bloom and largely dependent on the wind speed and direction. For example, strong northeasterly winds can temporarily reverse the flow on the shelf from the north to the south (Pickart et al., 2011), substantially lengthening the mean residence time (Winsor & Chapman, 2004). The assumption used above to compute the NCP is that the water remains largely stationary for the 2 month period between mid-May and mid-July. The climatological mean winds during this time of year tend to be moderately out of the northeast (Lin et al., 2016), which suggests an average residence time in the middle of the range suggested by the above models of ~4 months. This is consistent with the observations of Nobre et al. (2016), who suggest that the last of the WW exits the Chukchi Shelf through Barrow Canyon by early September, giving a flushing time of 3.5 months (mid-May to early September) for our domain. This, in turn, implies that up to 50% of the water typically sampled in our study region in mid-July emanated from south of the domain.

6. Conclusions

Given the relatively short duration of the phytoplankton bloom and the longer residence time for water on the shelf, our results suggest that accurate estimates of NCP in the northeastern Chukchi Sea require prebloom measurements of NO_3^- from no farther away than the southern portion of the Chukchi Sea. While such measurements are currently lacking, there is little reason to think that the NO_3^- levels there would be substantially different from those we measured during SUBICE. Fortunately, future cruises to the Chukchi Sea by the international research community, perhaps as part of the ongoing Distributed Biological Observatory program (Grebmeier et al., 2010, 2015), should increase the number of prebloom nutrient samples available for assessment of NCP and other biogeochemical processes in this highly productive and rapidly changing sector of the Arctic Ocean.

The high prebloom nutrient concentrations observed throughout the northeastern Chukchi Sea shelf during SUBICE provide critical information for evaluating the potential of these shelf systems to support phytoplankton growth under both ice-free and ice-covered conditions. Recent cruises to the same general area as that sampled during SUBICE demonstrated that phytoplankton could attain extremely high concentrations beneath the sea ice on the Chukchi Sea shelf (Arrigo et al., 2012, 2014). Obviously, these intense underice phytoplankton blooms required high prebloom nutrient concentrations to reach the extraordinary biomass levels that were observed (Zhang et al., 2015). However, there was little information about prebloom nutrient inventories at that time, so the possible extent of these blooms had been impossible to determine. Results presented here show that ice-covered waters throughout most of the northeastern Chukchi Sea have sufficient prebloom nutrients to support widespread growth of phytoplankton beneath the sea ice, consistent

with previous modeling results (Zhang et al., 2015). Therefore, once the snow melts and melt ponds form in spring, increased light transmission through the sea ice to the waters below the ice (Frey et al., 2011) could fuel large phytoplankton blooms over a much wider area than previously thought. The ecological implications of these blooms are currently unknown but are likely to be substantial.

Acknowledgments
We thank the captain and crew of the USCGC *Healy* and the SUBICE scientific team. This research was sponsored by the NSF Office of Polar Programs (PLR-1304563 to K. R. A. and PLR-1303617 to R. S. P.). Data are available from the Dryad Digital Repository: https://doi.org/10.5061/dryad.fm7b5.

References

Aagaard, K., & Roach, A. T. (1990). Arctic ocean-shelf exchange: Measurements in Barrow Canyon. *Journal of Geophysical Research*, *95*, 18,163–18,175.

Alkire, M. B., D'Asaro, E., Lee, C., Perry, M. J., Gray, A., Cetinic, I., … Gonzalez-Posada, A. (2012). Estimates of net community production and export using high-resolution, Lagrangian measurements of O_2, NO_3^-, and POC through the evolution of a spring diatom bloom in the North Atlantic. *Deep-Sea Research, Part I*, *64*, 157–174.

Anderson, L. G., Andersson, P. S., Björk, G., Peter Jones, E., Jutterström, S., & Wåhlström, I. (2013). Source and formation of the upper halocline of the Arctic Ocean. *Journal of Geophysical Research, Oceans*, *118*, 410–421. https://doi.org/10.1029/2012JC008291

Armstrong, F., Stearns, C. R., & Strickland, J. (1967). The measurement of upwelling and subsequent biological process by means of the Technicon Autoanalyzer® and associated equipment. *Deep Sea Research*, *14*, 381–389. https://doi.org/10.1016/0011-7471(67)90082-4

Arrigo, K. R., & van Dijken, G. L. (2011). Secular trends in Arctic Ocean net primary production. *Journal of Geophysical Research*, *116*, C09011. https://doi.org/10.1029/2011JC007151

Arrigo, K. R., & van Dijken, G. L. (2015). Continued increases in Arctic Ocean primary production. *Progress in Oceanography*, *136*, 60–70. https://doi.org/10.1016/j.pocean.2015.05.002.u

Arrigo, K. R., Perovich, D. K., Pickart, R. S., Brown, Z. W., van Dijken, G. L., Lowry, K. E., … Swift, J. H. (2012). Massive phytoplankton blooms under Arctic sea ice. *Science*, *336*, 1408.

Arrigo, K. R., Perovich, D. K., Pickart, R. S., Brown, Z. W., van Dijken, G. L., Lowry, K. E., … Swift, J. H. (2014). Phytoplankton blooms beneath the sea ice in the Chukchi Sea. *Deep-Sea Research Part II*, *105*, 1–16. https://doi.org/10.1016/j.dsr2.2014.03.018

Belanger, S., Babin, M., & Tremblay, J.-E. (2013). Increasing cloudiness in Arctic damps the increase in phytoplankton primary production due to sea ice receding. *Biogeosciences*, *10*, 4087–4101.

Bourke, R. H., & Paquette, R. G. (1976). Atlantic water on the Chukchi Shelf. *Geophysical Research Letters*, *3*, 629–632. https://doi.org/10.1029/GL003i010p00629

Brown, Z. W., Lowry, K., Palmer, M. A., van Dijken, G. L., Mills, M. M., Pickart, R. S., & Arrigo, K. R. (2015a). Characterizing the subsurface chlorophyll a maximum in the Chukchi Sea and Canada Basin. *Deep-Sea Research Part II*, *118*, 88–104.

Brown, Z. W., Casciotti, K. L., Pickart, R. S., Swift, J. H., & Arrigo, K. R. (2015b). Aspects of the marine nitrogen cycle of the Chukchi Sea shelf and Canada Basin. *Deep-Sea Research Part II*, *118*, 73–87.

Carmack, E. C. (2000). The Arctic Ocean's freshwater budget: Sources, storage and export. In E. L. Lewis et al. (Eds.), *The Freshwater Budget of the Arctic Ocean* (pp. 91–126). The Netherlands: Kluwer Academic Publishers.

Carmack, E. C., & Wassmann, P. (2006). Food-webs and physical biological coupling on pan-Arctic shelves: Perspectives, unifying concepts and future research. *Progress in Oceanography*, *71*, 446–477.

Cavalieri, D. J., Parkinson, C. L., Gloersen, P., & Zwally, H. J. (1996). Sea ice concentrations from Nimbus-7 SMMR and DMSP SSM/I-SSMIS passive microwave data, version 1. Boulder, Colorado USA, NASA National Snow and Ice Data Center Distributed Active Archive Center. https://doi.org/10.5067/8GQ8LZQVL0VL.

Chang, B. X., & Devol, A. H. (2009). Seasonal and spatial patterns of sedimentary denitrification rates in the Chukchi Sea. *Deep-Sea Research Part II*, *56*, 1339–1350.

Coachman, L. K., Aagaard, K., & Tripp, R. B. (1975). *Bering Strait, the Regional Physical Oceanography* (pp. 172). Seattle: Univ. of Washington Press.

Codispoti, L. A., Flagg, C. N., Kelly, V., & Swift, J. H. (2005). Hydrographic conditions during the 2002 SBI process experiments. *Deep-Sea Research Part II*, *52*, 3199–3226.

Codispoti, L. A., Flagg, C. N., & Swift, J. H. (2009). Hydrographic conditions during the 2004 SBI process experiments. *Deep-Sea Research Part II*, *56*(17), 1144–1163.

Codispoti, L. A., Kelly, V., Thessen, A., Matrai, P., Suttles, S., Hill, V., … Light, B. (2013). Synthesis of primary production in the Arctic Ocean: III. Nitrate and phosphate based estimates of net community production. *Progress in Oceanography*, *110*, 126–150.

Cooper, L. W., Whitledge, T. E., Grebmeier, J. M., & Weingartner, T. (1997). The nutrient, salinity, and stable oxygen isotope composition of Bering and Chukchi Seas waters in and near Bering Strait. *Journal of Geophysical Research*, *102*, 12,563–12,573.

Danielson, S. A., Eisner, L., Ladd, C., Mordy, C., Sousa, L., & Weingartner, T. J. (2017). A comparison between late summer 2012 and 2013 water masses, macronutrients, and phytoplankton standing crops in the northern Bering and Chukchi Seas. *Deep-Sea Research Part II*, *135*, 7–26.

Devol, A. H., Codispoti, L. A., & Christensen, J. P. (1997). Summer and winter denitrification rates in western Arctic shelf sediments. *Continental Shelf Research*, *17*, 1029–1033. https://doi.org/10.1016/S0278-4343(97)00003-4

Eppley, R. W., & Peterson, B. J. (1979). Particulate organic-matter flux and planktonic new production in the deep ocean. *Nature*, *282*(5740), 677–680.

Frey, K. E., Perovich, D. K., & Light, B. (2011). The spatial distribution of solar radiation under a melting Arctic sea ice cover. *Geophysical Research Letters*, *38*, L22501. https://doi.org/10.1029/2011GL049421

Granger, J., Prokopenko, M. G., Sigman, D. M., Mordy, C. W., Morse, Z. M., Morales, L. V., … Plessen, B. (2011). Coupled nitrification-denitrification in sediment of the eastern Bering Sea shelf leads to ^{15}N enrichment of fixed N in shelf waters. *Journal of Geophysical Research*, *116*, C11006. https://doi.org/10.1029/2010JC006751

Grebmeier, J. M., Moore, S. E., Overland, J. E., Frey, K. E., & Gradinger, R. (2010). Biological response to recent Pacific Arctic sea ice retreats. *Eos, Transaction*, *91*(18), 161–162.

Grebmeier, J. M., Bluhm, B. A., Cooper, L. W., Danielson, S. L., Arrigo, K. R., Blanchard, A. L., …, Okkonen, S. R. (2015). Ecosystem characteristics and processes facilitating persistent macrobenthic biomass hotspots and associated benthivory in the Pacific Arctic. *Progress in Oceanography*, *136*, 92–114. https://doi.org/10.1016/j.pocean.2015.05.006

Haines, J. R., Atlas, R. M., Griffiths, R. P., & Morita, R. Y. (1981). Denitrification and nitrogen fixation in Alaskan continental-shelf sediments. *Applied and Environmental Microbiology*, *41*, 412–421.

Hansell, D. A., Whitledge, T. E., & Goering, J. J. (1993). Patterns of nitrate utilization and new production over the Bering-Chukchi Shelf. *Continental Shelf Research*, *13*, 601–527.

Hartnett, H. (1998). Organic carbon input, degradation and preservation in continental margin sediments: An assessment of the role of a strong oxygen deficient zone, Univ. of Wash., Seattle.

Henriksen, K., Blackburn, T. H., Lomstein, B. A., & McRoy, C. P. (1993). Rates of nitrification, distribution of nitrifying bacteria and inorganic N fluxes in northern Bering Chuckchi Shelf sediments. *Continental Shelf Research*, *13*, 629–651. https://doi.org/10.1016/0278-4343(93)90097-H

Hessen, D. O., Frigstad, H., Faerovig, P. J., Wojewodzic, M. W., & Leu, E. (2012). UV radiation and its effects on P-uptake in arctic diatoms. *Journal of Experimental Marine Biology and Ecology*, *411*, 45–51.

Holm-Hansen, O., Lorenzen, C. J., Holmes, R. W., & Strickland, J. D. H. (1965). Fluorometric determination of chlorophyll. *ICES Journal of Marine Science*, *30*(1), 3–15. https://doi.org/10.1093/icesjms/30.1.3

Koike, I., & Hattori, A. (1979). Estimates of denitrification in sediments of the Bering Sea shelf. *Journal of Geophysical Research*, *26*, 409–415.

Lin, P., Pickart, R. S., Stafford, K. M., Moore, G. W. K., Torres, D. J., Bahr, F., & Hu, J. (2016). Seasonal variations in the Beaufort shelfbreak jet and its relationship to Arctic cetacean occurrence. *Journal of Geophysical Research, Oceans*, *121*, 8434–8454. https://doi.org/10.1002/2016JC011890

Lowry, K. E., Pickart, R. S., Mills, M. M., Brown, Z. W., van Dijken, G. L., Bates, N. R., & Arrigo, K. R. (2015). The influence of winter water on phytoplankton blooms in the Chukchi Sea. *Deep-Sea Research Part II*, *118*, 53–72.

Martin, J., Tremblay, J.-É., Gagnon, J., Tremblay, G., Lapoussière, A., Jose, C., … Michel, C. (2010). Prevalence, structure and properties of subsurface chlorophyll maxima in Canadian Arctic waters. *Marine Ecology Progress Series*, *412*, 69–84. https://doi.org/10.3354/meps08666

Mills, M. M., Brown, Z. W., Lowry, K. E., van Dijken, G. L., Becker, S., Pal, S., … Arrigo, K. R. (2015). Impacts of low phytoplankton NO_3^-:PO_4^{3-} utilization ratios over the Chukchi Shelf, Arctic Ocean. *Deep-Sea Research Part II*, *118*, 105–121. https://doi.org/10.1016/j.dsr2.2015.02.007

Nobre, C., Pickart, S., Moore, G. W. K., Ashjian, C. J., Arrigo, K. R., Grebmeier, J. M., … He, J. (2016). Seasonal to mesoscale variability of water masses in Barrow Canyon, Chukchi Sea, *Eos, Transactions American Geophysical Union*, Abstract HE54A-1554.

Pacini, A., Pickart, R. S., Moore, G. W. K., & Våge, K. (2016). Hydrographic structure and modification of Pacific winter water on the Chukchi Sea shelf in late spring, *Eos, Transactions American Geophysical Union*, Abstract H14B-1406.

Padman, L., & Erofeeva, S. (2004). A barotropic inverse tidal model for the Arctic Ocean. *Geophysical Research Letters*, *31*, L02303. https://doi.org/10.1029/2003GL019003

Pickart, R. S., Moore, G. W. K., Torres, D. J., Fratantoni, P. S., Goldsmith, R. A., & Yang, J. (2009). Upwelling on the continental slope of the Alaskan Beaufort Sea: Storms, ice, and oceanographic response. *Journal of Geophysical Research*, *114*, C00A13. https://doi.org/10.1029/2008JC005009

Pickart, R. S., Spall, M. A., Moore, G. W. K., Weingartner, T. J., Woodgate, R. A., Aagaard, K., & Shimada, K. (2011). Upwelling in the Alaskan Beaufort Sea: Atmospheric forcing and local versus non-local response. *Progress in Oceanography*. https://doi.org/10.1016/j.pocean.2010.11.005

Pickart, R. S., Moore, G. W. K., Mao, C., Bahr, F., Nobre, C., & Weingartner, T. J. (2016). Circulation of winter water on the Chukchi Shelf in early summer. *Deep-Sea Research Part II*, *130*(C), 56–75. https://doi.org/10.1016/j.dsr2.2016.05.001

Sambrotto, R. N., Goering, J. J., & McRoy, C. P. (1984). Large yearly production of phytoplankton in the western Bering Strait. *Science*, *225*, 1147–1150.

Spall, M. A. (2007). Circulation and water mass transformation in a model of the Chukchi Sea. *Journal of Geophysical Research*, *112*, C05025. https://doi.org/10.01029/02005JC002264

Springer, A. M., & McRoy, C. P. (1993). The paradox of pelagic food webs in the northern Bering Sea. III. Patterns of primary production. *Continental Shelf Research*, *13*, 575–579.

Tanaka, T., Guo, L. D., Deal, C., Tanaka, N., Whitledge, T., & Murata, A. (2004). N deficiency in a well-oxygenated cold bottom water over the Bering Sea shelf: Influence of sedimentary denitrification. *Continental Shelf Research*, *24*, 1271–1283. https://doi.org/10.1016/j.csr.2004.04.004

Varela, D. E., Crawford, D. W., Wrohan, I. A., Wyatt, S. N., & Carmack, E. C. (2013). Pelagic primary productivity and upper ocean nutrient dynamics across Subarctic and Arctic Seas. *Journal of Geophysical Research, Oceans*, *118*, 7132–7152. https://doi.org/10.1002/2013JC009211

Walsh, J. J., McRoy, C. P., Coachman, L. K., Goering, J. J., Nihoul, J. J., Whitledge, T. E., … Dean, K. (1989). Carbon and nitrogen cycling within the Bering/Chukchi Seas: Source regions for organic matter effecting AOU demands of the Arctic Ocean, *Progress in Oceanography*, *22*, 277–359.

Wang, J., Cota, G. F., & Comiso, J. C. (2005). Phytoplankton in the Beaufort and Chukchi Seas: Distribution, dynamics, and environmental forcing. *Deep-Sea Research, Part II*, *52*(24–26), 3355–3368.

Weingartner, T. J., Aagaard, K., Woodgate, R., Danielson, S., Sasaki, Y., & Cavalieri, D. J. (2005). Circulation on the north central Chukchi Sea shelf. *Deep-Sea Research Part II*, *52*, 3150–3174.

Weingartner, T. J., Dobbins, E., Danielson, S., Winsor, P., Potter, R., & Statscewich, H. (2013). Hydrographic variability over the northeastern Chukchi Sea shelf in summer-fall 2008–2010. *Continental Shelf Research*, *67*, 5–22.

Winsor, P., & Chapman, D. C. (2004). Pathways of Pacific water across the Chukchi Sea: A numerical model study. *Journal of Geophysical Research*, *109*, C03002. https://doi.org/10.1029/2003JC001962

Woodgate, R. A., Aagaard, K., & Weingartner, T. J. (2006). Interannual changes in the Bering Strait fluxes of volume, heat and freshwater between 1991 and 2004. *Geophysical Research Letters*, *33*, L15609. https://doi.org/10.1029/2006GL026931

Zhang, J., Spitz, Y. H., Steele, M., Ashjian, C., Campbell, R., Berline, L., & Matrai, P. (2010). Modeling the impact of declining sea ice on the Arctic marine planktonic ecosystem. *Journal of Geophysical Research*, *115*, C10015. https://doi.org/10.1029/2009JC005387

Zhang, J., Ashjian, C. J., Campbell, R., & Spitz, Y. H. (2015). The influence of sea ice and snow cover and nutrient availability on the formation of massive under-ice phytoplankton blooms in the Chukchi Sea. *Deep-Sea Research Part II*, *118*, 122–135. https://doi.org/10.1016/j.dsr2.2015.02.008